Applied Mathematics & Information Sciences
An International Journal

http://dx.doi.org/10.18576/amis/170613

Exploring local quantum Fisher information beyond entanglement of two distant qubits in coupled dissipative cavities via a Waveguide

Abdel-Baset A. Mohamed

Department of Mathematics, College of Science and Humanities, Prince Sattam bin Abdulaziz University, Al-Kharj, Saudi Arabia

Received: 2 Oct. 2023, Revised: 26 Oct. 2023, Accepted: 28 Oct. 2023
Published online: 1 Nov. 2023

Abstract: We explore local quantum Fisher information (QFI) and concurrence entanglement of two distant qubits. Each qubit interacts separately with a dissipative cavity, and the two cavities are coupled via an optical fiber. Under increasing the cavity-atom, fiber-cavity, and cavity dissipation couplings, the generation and robustness of the atomic local quantum Fisher information and concurrence quantum information resources are investigated. The frequencies, regularity, and amplitudes of the generated atomic local quantum Fisher information and entanglement can be enhanced while the time disappearance-entanglement intervals are reduced by increasing the fiber-cavity interactions in the presence of the strong cavity-atom couplings. It is shown that The time disappearance-entanglement intervals depend on the fiber-cavity and the cavity-atom interaction couplings. The robustness dynamics of the initial maximal coherence's local quantum Fisher information and the maximal entanglement's concurrence can be enhanced by increasing the fiber-cavity coupling. It is found that, in the study cases of the generation and robustness of the local quantum Fisher information and entanglement, the stability of the Local QFI growth and the concurrence degradation (due to the cavity dissipation effects) depend on the atom-cavity, fiber-cavity, and cavity dissipation couplings.

Keywords: local quantum Fisher information; Cavity damping; Optical fiber.

1 Introduction

Generation quantum coherence and quantum entanglement are distinctive tools and remarkable resources for quantum information [1]. Quantum coherence is not only an embodiment of the superposition principle of states but also the basis of many unique phenomena in quantum optics, including: entanglement and steerability. It is at the heart of quantum information and quantum optics since the foundational works [2]. Several rigorous concepts and tools have been introduced in quantum resource theory to explore quantum coherence [3,4,5]. Various quantum information processing tasks were implemented by utilizing the quantum coherence, including: quantum computing [6], information storage[7], communication [8], and quantum metrology [9]. Therefore, generating quantum coherence in different quantum systems is important both for the physical fundamental research and the quantum technology.

In closed/open two-qubit systems, the quantum coherence (as entanglement, coherence loss) were investigated via different several quantifiers, as: von Neumann entropy [10,11], concurrence, negativity [12, 13,14,15,16], skew-information quantity quantifiers [17] (local uncertainty [18] and uncertainty-induced non-locality [19]), quantum Jensen-Shannon divergence [20,21] and quantum Fisher information (QFI) [22,23]. QFI is used to quantify the the parameter estimation protocol optimal accuracy [24]. Local quantum Fisher information (local QFI) [25,26] is based on the minimal quantum Fisher information and its coherence has been proposed as another information resource beyond entanglement. In open systems, local QFI is used to measure quantum correlation beyond entanglement while in closed systems itis used to measure quantum coherence. Local QFI has recently been used a for quantifying two-qubit coherence in different systems, as: two-qubit local QFI beyond entanglement was investigated for a nonlinear generalized cavity with an intrinsic decoherence [27] and in in two-qubit Ising model with an arbitrary magnetic field [28]. The

* Corresponding author e-mail: abdelbastm@aun.edu.eg

spontaneous emergence of local QFI beyond entanglement was explored in a noisy two-qubit Heisenberg model with Dzyaloshinskii-Moria and Kaplan-Shekhtman-Entin-Wohlman-Aharony interactions [29,30], Heisenberg XYZ chain with Dzyaloshinskii Moriya interactions [31] and in two cat states carrying equal gravitational charges [32].

Exploring the generation of two-qubit coherence resources in real two-qubit models become a useful work field for advancing quantum computing [1] and estimation [33]. The cavity-qubit system models, in which the cavities are coupled by an optical fibers have potential applications to design quantum networks and communication [34,35]. The isolated qubit-cavity systems were used to implement quantum gates [36] and generated entangled state [37,38,39].

In open systems, the models have problems of losing of the quantum coherence and entanglement, this is due to the qubit-cavity interactions with the external environment, where their quantum information resources are affected by the external dissipations [40,41,42]. In closed cavity-fiber-cavity systems, the entanglement were studied [43,44,45], each cavity interacting with a qubit/qutrit. The generation of coherence resources (as, local quantum Fisher information and entanglement) is very limited and have several attentions in open systems. Therefore, in this work, we will explore local quantum Fisher information and concurrence entanglement of two distant qubits in coupled dissipative cavities via an optical fiber under increasing couplings of the cavity-atom interaction, fiber-cavity interaction, and cavity dissipation coupling.

In this paper, the atom-cavity-fiber physical model and its master motion equation are introduced in Sec. II. While the coherence local QFI and entanglement measures will be introduced in Sec. III. The discussion of the generation and robustness of the atomic local QFI and concurrence quantum information resources will be investigated in Sec. IV. In Sec. V, conclusion is written.

2 The atom-cavity-fiber physical model

The model consists of two two-level distant atoms (A and B qubits). Each one of qubits (has up $|1_k\rangle$ and down $|0_k\rangle$ states) interacts resonantly with a dissipative cavity field with the same frequency ω. The two dissipative cavities (A and B fields) are coupled via an optical fiber (has up $|1_f\rangle$ and down $|0_f\rangle$ states). At zero temperature, the dynamics of the two dissipative cavity-qubit systems is given by the master equation's cavity damping, [46,47]

$$\frac{\partial \hat{R}}{\partial t} = -i[\hat{H},\hat{R}] + \sum_{k=A,B} \gamma_k (2\hat{a}_k \hat{R} \hat{a}_i^\dagger - \hat{a}_k^\dagger \hat{a}_k \hat{R} - \hat{R}\hat{a}_k^\dagger \hat{a}_k). \quad (1)$$

where $\hat{R}(t)$ is the density matrix's time-dependent (cavity-atom)-fiber-(cavity-atom) states. γ_k are the k-cavity dissipation constants. The function represents the interaction (cavity-atom)-fiber-(cavity-atom) Hamiltonian, that is given by

$$\hat{H}_{int} = \sum_{k=A,B} \{\xi_i(\hat{a}_i^\dagger |0_k\rangle\langle 1_k + \hat{a}_i |1_k\rangle\langle 0_k) + \xi_f(\hat{b}\hat{a}_k^\dagger + \hat{b}^\dagger \hat{a}_k)\}. \quad (2)$$

Here $\hat{a}_i^\dagger$ and $\hat{a}_i$ are the cavity-fields raising and lowering operators, whereas $\hat{b}$ is the lower fiber-field operator. The $\xi_k (k = A,B)$ and ξ_f are the atom-cavity and fiber-cavity interaction couplings, respectively.

Here, we find the general solution of the master equation (Eq.1)in the weak pumping regime. In this regime, we consider that the excitation and the dissipation are sufficiently small, therfore the off-diagonal terms of Eq.1 $(2\hat{a}_i \hat{R} \hat{a}_i^\dagger)$ can be neglected [47,48], and Eq.1 becomes

$$i\frac{d}{dt}\hat{R} = \hat{H}_{non}\hat{R} - (\hat{R}\hat{H}_{non})^\dagger. \quad (3)$$

The non-Hermitian operator $\hat{H}_{non}$ has the following expression:

$$H_{non} = \hat{H}_{int} - i\gamma_A \hat{a}_A^\dagger \hat{a}_A - i\gamma_B \hat{a}_B^\dagger \hat{a}_B. \quad (4)$$

Therefore the dynamics of the two dissipative cavity-qubit systems of Eq.1 can be described by

$$\frac{d}{dt}|\Psi(t)\rangle = -i\hat{H}_{non}|\Psi(t)\rangle. \quad (5)$$

The wave function is given by:

$$|\Psi(t)\rangle = |V_1\rangle \otimes |0_A 0_B\rangle + |V_2\rangle \otimes |0_A 1_B\rangle + |V_3\rangle \otimes |1_A 0_B\rangle + |V_4\rangle \otimes |1_A 1_B\rangle. \quad (6)$$

In the basis space of the two cavities-fiber field staes, $|C_A, C_B, Fiber\rangle$: $\{|000\rangle, |001\rangle, |010\rangle, |011\rangle, |100\rangle, |101\rangle, |110\rangle, |111\rangle\}$, then the states $|V_i\rangle$ are given by

$$\begin{aligned}
|V_1\rangle &= F_1|000\rangle + F_5|001\rangle + F_9|010\rangle + F_{13}|011\rangle + F_{17}|100\rangle \\
&\quad + x_{21}|101\rangle + F_{25}|110\rangle + X_{29}|111\rangle, \\
|V_2\rangle &= x_2|000\rangle + x_6|001\rangle + x_{10}|010\rangle + x_{14}|011\rangle + x_{18}|100\rangle \\
&\quad + x_{22}|101\rangle + x_{26}|110\rangle + x_{30}|111\rangle, \\
|V_3\rangle &= x_3|000\rangle + x_7|001\rangle + x_{11}|010\rangle + x_{15}|011\rangle + x_{19}|100\rangle \\
&\quad + x_{23}|101\rangle + x_{27}|110\rangle + x_{31}|111\rangle, \quad (7) \\
|V_4\rangle &= x_4|000\rangle + x_8|001\rangle + x_{12}|010\rangle + x_{16}|011\rangle + x_{20}|100\rangle \\
&\quad + x_{24}|101\rangle + x_{28}|110\rangle + x_{32}|111\rangle.
\end{aligned}$$

The amplitudes $F_n(n=1-32)$ are derived from Eq.5 and they verify the following differential equations:

$$
\begin{aligned}
\dot{F}_2 &= -i\xi_B F_9,\\
\dot{F}_3 &= -i\xi_A F_{17},\\
\dot{F}_4 &= -i\xi_A F_{18} - i\xi_B F_{11},\\
\dot{F}_5 &= -i\xi_f F_9 - i\xi_f F_{17},\\
\dot{F}_6 &= -i\xi_B F_{13} - i\xi_f F_{10} - i\xi_f F_{18},\\
\dot{F}_7 &= -i\xi_A F_{21} - i\xi_f F_{11} - i\xi_f F_{19},\\
\dot{F}_8 &= -i\xi_A F_{22} - i\xi_B F_{15} - i\xi_f F_{12} - i\xi_f F_{20},\\
\dot{F}_9 &= -i\xi_B F_2 - i\xi_f F_5 - \gamma_B F_9,\\
\dot{F}_{10} &= -i\xi_f F_6 - \gamma_B F_{10},\\
\dot{F}_{11} &= -i\xi_A F_{25} - i\xi_B F_4 - i\xi_f F_7 - \gamma_B F_{11},\\
\dot{F}_{12} &= -i\xi_A F_{26} - i\xi_f F_8 - \gamma_B F_{12},\\
\dot{F}_{13} &= -i\xi_B F_6 - i\xi_f F_{25} - \gamma_B F_{13},\\
\dot{F}_{14} &= -i\xi_f F_{26} - \gamma_B F_{14},\\
\dot{F}_{15} &= -i\xi_A F_{29} - i\xi_B F_8 - i\xi_f F_{27} - \gamma_B F_{15},\\
\dot{F}_{16} &= -i\xi_A F_{30} - i\xi_f F_{28} - \gamma_B F_{16},\\
\dot{F}_{17} &= -i\xi_A F_3 - i\xi_f F_5 - \gamma_A F_{17},\\
\dot{F}_{18} &= -i\xi_A F_4 - i\xi_B F_{25} - i\xi_f F_6 - \gamma_A F_{18},\\
\dot{F}_{19} &= -i\xi_f F_7 - \gamma_A F_{19}\\
\dot{F}_{20} &= -i\xi_B F_{27} - i\xi_f F_8 - \gamma_A F_{20},\\
\dot{F}_{21} &= -i\xi_A F_7 - i\xi_f F_{25} - \gamma_A F_{21},\\
\dot{F}_{22} &= -i\xi_A F_8 - i\xi_B F_{29} - i\xi_f F_{26} - \gamma_A F_{22},\\
\dot{F}_{23} &= -i\xi_f F_{27} - \gamma_A F_{23},\\
\dot{F}_{24} &= -i\xi_B F_{31} - i\xi_f F_{28} - \gamma_A F_{24},\\
\dot{F}_{25} &= -i\xi_A F_{11} - i\xi_B F_{18} - i\xi_f F_{13} - i\xi_f F_{21} - (\gamma_A+\gamma_B)F_{25},\\
\dot{F}_{26} &= -i\xi_A F_{12} - i\xi_f F_{14} - i\xi_f F_{22} - (\gamma_A+\gamma_B)F_{26},\\
\dot{F}_{27} &= -i\xi_B F_{20} - i\xi_f F_{15} - i\xi_f F_{23} - (\gamma_A+\gamma_B)F_{27},\\
\dot{F}_{28} &= -i\xi_f F_{16} - i\xi_f F_{24} - (\gamma_A+\gamma_B)F_{28},\\
\dot{F}_{29} &= -i\xi_A F_{15} - i\chi_B F_{22} - (\gamma_A+\gamma_B)F_{29},\\
\dot{F}_{30} &= -i\xi_A F_{16} - (\gamma_A+\gamma_B)F_{30},\\
\dot{F}_{31} &= -i\xi_B F_{24} - (\gamma_A+\gamma_B)F_{31},
\end{aligned}
\tag{8}
$$

where also, $F_1(t) = F_1(0)$ and $F_{32}(t) = F_{32}(0)e^{-(\gamma_A+\gamma_B)t}$. In the atomic space sates: $\{|S_1\rangle = |0_A 0_B\rangle, |S_2\rangle = |1_A 0_B\rangle, |S_3\rangle = |0_A 1_B\rangle, |S_4\rangle = |1_A 1_B\rangle\}(k = 1-4)$, the atomic reduced density matrix is given by

$$
\hat{R}^{AB}(t) = \sum_{i,j=1}^{4} \langle V_i|V_j\rangle |S_i\rangle\langle S_j|, \tag{9}
$$

That uses to investigate the generation and robustness of the atomic local QFI and concurrence quantum information resources.

3 local QFI Coherence and entanglement measures

The considered two-qubit local QFI and concurrence entanglement quantifiers are

– Local quantum Fisher information (local QFI): Here, local QFI is used to quantify the quantum correlation in the presence of the two-cavity dissipations whereas in the presence of the two-cavity dissipations it used to quantify quantum coherence (purity loss). Local QFI is the minimum of the QFI [25] calculated by an one qubit local unitary evolution of the two qubits. The local QFI is given by [25,26]

$$
L(t) = 1 - \max\{\lambda_1, \lambda_2, \lambda_3\}, \tag{10}
$$

$\{\lambda_k\}(k = 1,2,3)$ are the symmetric matrix $S = [s_{ij}](i,j = 1,2,3)$ eigenvalues. The elements' of the symmetric matrix depend on the eigenvalues $\xi_k(k = 1,2,3,k)$ and eigenstates Λ_k of the atomic density matrix $R^{AB}(t)$, as:

$$
s_{ij} = \sum_{\xi_m+\xi_n\neq 0} \frac{2\xi_m\xi_n}{\xi_m+\xi_n} T^i_{mn} T^{j\dagger}_{nm}, \tag{11}
$$

$T^j_{mn} = \langle\Lambda_m|\hat{H}_i|\Lambda_n\rangle$ and $\hat{H}_i = I\otimes\sigma_i$ with the Pauli matrices $\sigma_i(i = 1,2,3)$. $L(t) = 1$ for a maximally entangled state. While if local QFI has zero-value, then the state $R(t)$ has no correlation.

–Concurrence entanglement: To compare the atomic local QFI dynamics with the generated two-atom entanglement dynamics, the concurrence is used to calculate the entanglement [14],

$$
C(t) = \max\{0, \sqrt{e_1} - \sqrt{e_2} - \sqrt{e_3} - \sqrt{e_4}\}, \tag{12}
$$

$e_i > e_{i+1}(i = 1-4)$ are the eigenvalues of the matrix: $X = R^{AB}(t)(\sigma_y\otimes\sigma_y)R^{AB*}(t)(\sigma_y\otimes\sigma_y)$. When $C(t) = 0$, the atomic state is disentangled state. $C(t) = 1$ for a maximally entangled state.

In the following, we use the time dependent atomic local QFI and concurrence function to explore the generated coherence's local QFI and entanglement's concurrence under the effects of the couplings of the cavity-atom interaction, fiber-cavity interaction, and cavity dissipation.

4 Atomic local QFI and concurrence dynamics

Under increasing couplings of the cavity-atom interaction ξ_i, fiber-cavity interaction α, and cavity dissipation coupling γ , the generation and robustness of the atomic local QFI and concurrence quantum information resources will be investigated. Our aim in this work is: (1) exporting the ability of the atom-cavity and fiber-cavity

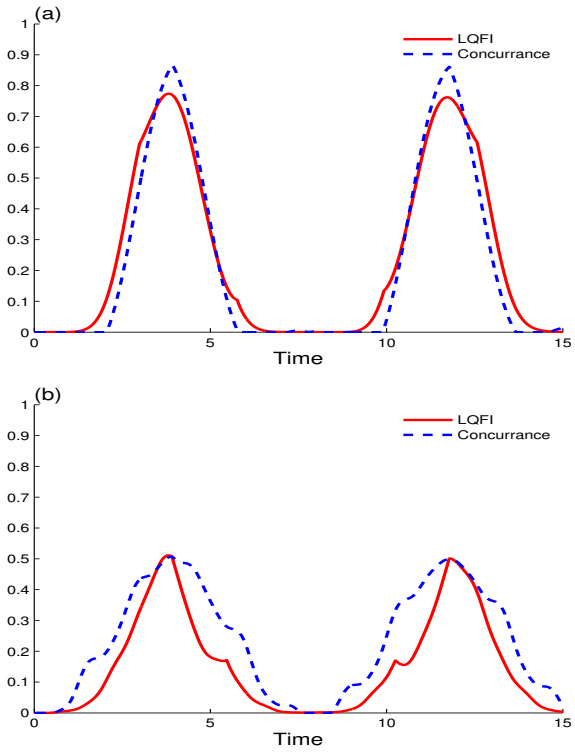

Fig. 1: The dynamics of the atomic local QFI and concurrence entanglement of the initial disentangled (cavity-atom)-fiber- (cavity-atom) state $|\psi(0)\rangle_{Pure}$ are shown for different fiber-cavity cases $\xi_f = 0.5$ in (a) and $\xi_f = 3$ in (b) with weak cavity-atom couplings $(\xi_A, \xi_B) = (0.4, 0.4)$ and dissipation couplings $\gamma_i = 0.0$.

interaction couplings to generate atomic local QFI and concurrence entanglement, we assume that the (cavity-atom)-fiber-(cavity-atom) system starts initially with the disentangled state: $|\psi(0)\rangle_{Pure} = |110\rangle \otimes |1_A 0_B\rangle$. (2) The robustness of a maximal initial coherence's local quantum Fisher information and entanglement's concurrence against the atom-cavity, fiber-cavity, and the two-cavity dissipation couplings. For this aim, the (cavity-atom)-fiber-(cavity-atom) system is initially in the maximally entangled state, $|\psi(0)\rangle_{Ent}$:

$$|\psi(0)\rangle_{Ent} = \frac{1}{16}[|V_2\rangle \otimes |0_A 1_B\rangle + |V_3\rangle \otimes |1_A 0_B\rangle]. \quad (13)$$

A- Generation of atomic local QFI and entanglement

In this case, we investigates the generation of the coherence's local QFI and entanglement's concurrence due to atom-cavity and fiber-cavity interactions, which they start with the disentangled state: $|\psi(0)\rangle_{Pure} = |110\rangle \otimes |1_A 0_B\rangle$. The initial reduced density matrix $|110\rangle \otimes |1_A 0_B\rangle\langle 110| \otimes \langle 1_A 0_B|$ does not present LQFI nor entanglement, i. e., $L(t) = C(t) = 0$. Figs. 1 and 3 show the capacity of the atom-cavity and fiber-cavity interaction couplings to generate coherence's local quantum Fisher information and entanglement's concurrence, and also show the cavity dissipation effects on the generated atomic LQFI and entanglement dynmaics. Here, we takes the atom-cavity ξ_i and fiber-cavity ξ_f couplings, i.e., the cavity-qubit couplings are smaller than the cavity-fiber coupling $\xi_f \geq \xi_i$ [49].

In Fig. 1a, the dynamics of the generation of the atomic coherence's local quantum Fisher information and entanglement's concurrence, due to weak cavity-atom couplings $(\xi_A, \xi_B) = (0.4, 0.4)$ are shown for the weak fiber-cavity interaction case of $\xi_f = 0.5$ in the absence of the two-cavity dissipation effects. After a specific time (this time is called "revival time of the atomic LQFI/entanglement"), the atomic coherence's local quantum Fisher information (non-suddenly) and entanglement's concurrence (suddenly) revivals and grows to its partial and maximal atomic coherence and entanglement. The atomic entanglement's concurrence exhibits a sudden disappearance and sudden reappearance phenomena. These phenomena of the sudden death and revival of the two-atom entanglement's concurrence happens, severally, at the ends of the time intervals of the entanglement's concurrence disappearance. The chosen weak couplings of the cavity-atom interaction and fiber-cavity interaction lead to generate atomic coherence's local quantum Fisher information and entanglement's concurrence periodically with regular oscillatory dynamics. The upper bounds of the concurrence are larger than those of the local QFI. From the atomic coherence's local QFI dynamics, we find that the generated atomic states can have partial coherence's LQFI during the time intervals of the entanglement's concurrence disappearance.

Fig. 1b illustrates the dynamics of the generated atomic coherence's local QFI (that changes, non-suddenly) and entanglement's concurrence of Fig. 1a for a strong weak fiber-cavity interaction coupling $\xi_f = 3$. In the cases of the Figs. 1(b,c), we observe that the strong weak fiber-cavity interaction coupling have a strong ability to generate two-qubit local QFI and concurrence information resources. The amplitudes's two-qubit local QFI and concurrence reduce while their frequencies, and regularity are improved. The time disappearance intervals of the entanglement's concurrence are reduced by increasing the fiber-cavity interaction coupling. During each time period, at the same time, the local QFI and concurrence can have maximal coherence and entanglement. The atomic coherence's local QFI exhibits a sudden-changes phenomena at different point. These phenomena of the sudden-changes points happens clear by increasing the fiber-cavity interaction coupling.

Fig. 2 shows the dynamics of the generated atomic local QFI and concurrence entanglement of Fig.1b for strong equal/unequal cavity-atom couplings (ξ_A, ξ_B). From Fig. 2a, for equal strong cavity-atom couplings

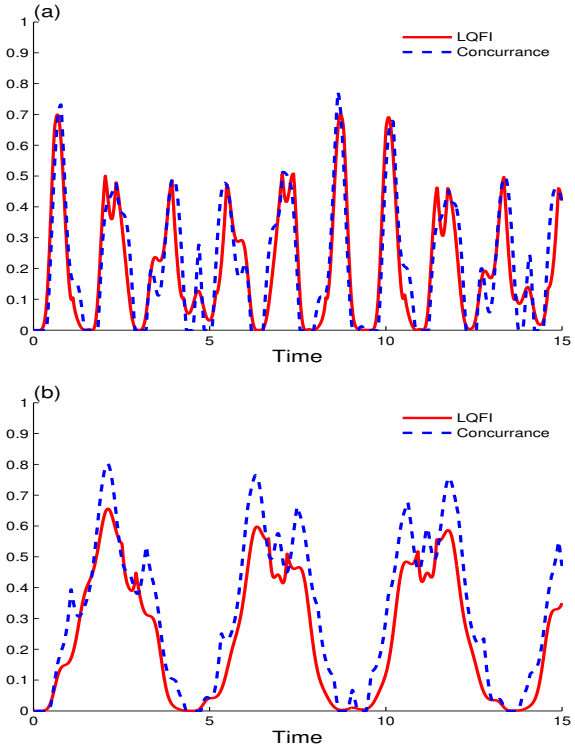

Fig. 2: The dynamics of the atomic local QFI and concurrence entanglement of Fig. 1b, but with strong cavity-atom couplings (ξ_A, ξ_B): equal cavity-atom couplings $(\xi_A, \xi_B) = (2, 2)$ in (b), and unequal cavity-atom couplings $(\xi_A, \xi_B) = (2, 0.4)$ in (b).

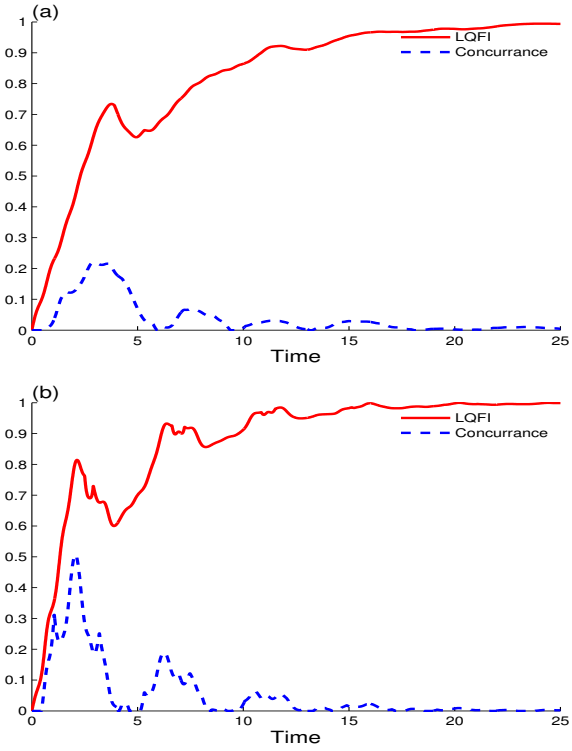

Fig. 3: The atomic local QFI and concurrence entanglement of Figs. 1b and 2b but with strong two-cavity dissipation couplings $\gamma_A = \gamma_B = 0.08$.

$(\xi_A, \xi_B) = (2, 2)$, we observe more irregular two-atom local QFI and concurrence oscillations with large amplitudes. The time disappearance intervals of the entanglement's concurrence are reduced by increasing the equal cavity-atom couplings. While the local QFI sudden-changes points increase clear. The revival time of the atomic local QFI/entanglement reduces, and they are generated, quickly. However, the regularity of the growth and the oscillations of the generated atomic local quantum Fisher information and concurrence entanglement depends on the cavity-atom interaction and fiber-cavity interactions. Fig. 2b illustrates that the frequencies, regularity, and amplitudes of the atomic local QFI and concurrence entanglement are enhanced by increasing the fiber-cavity interactions in the presence of the unequal cavity-atom interaction couplings. Also, the time disappearance intervals of the entanglement's concurrence are reduced.

Fig. 3 displays the dynamics of the atomic local QFI and concurrence entanglement of Figs. 1b and 2b under the effect of strong two-cavity dissipation couplings $\gamma_A = \gamma_B = 0.8$. Fig. 3a shows that, in this case of the strong two-cavity dissipation effects, the frequencies and amplitudes of concurrence reduce to have damped oscillatory dynamics. After a short time, the concurrence entanglement degrades and vanishes, completely, due to the two-cavity dissipation effects. While the atomic local quantum Fisher information grows to stabilizes at maximal atomic coherence. We find that the generated atomic states can have atomic maximal coherence of the LQFI during the time intervals of the entanglement's concurrence disappearance. The growth of the atomic coherence's local QFIand the degradation of the concurrence entanglement are shown in Fig. 3b under unequal strong cavity-atom couplings, which have ability to enhance the robustness (against the cavity dissipation) and the stability of the generated the growth of the LQFI and the degradation of the concurrence. The stability of the generated atomic maximal coherence of the LQFI depends on the atom-cavity, fiber-cavity, and cavity dissipation couplings.

B- Robustness of the initial maximal LQFI and entanglement

Here, we investigate the robustness dynamics of the maximal coherence's local quantum Fisher information

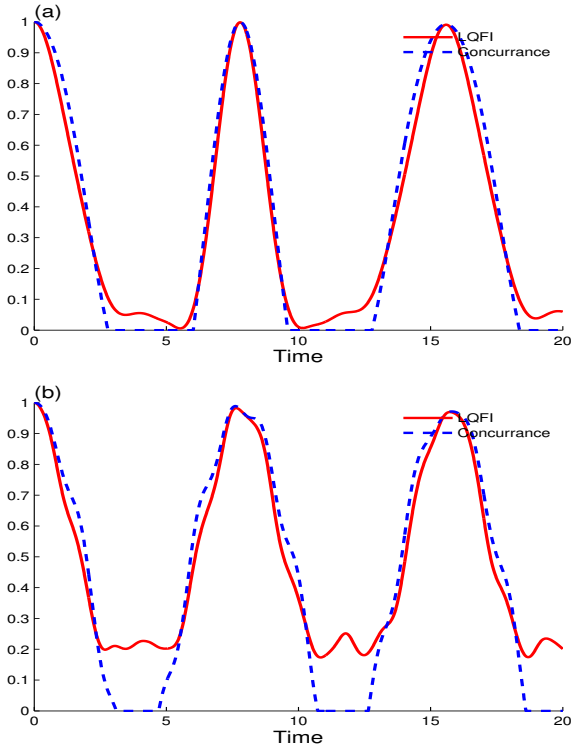

Fig. 4: The dynamics of the maximal coherence's local QFI and the maximal entanglement's concurrence of the initial maximally entangled state: $\frac{1}{16}[|V_2\rangle \otimes |0_A 1_B\rangle + |V_3\rangle \otimes |1_A 0_B\rangle]$ are shown for different fiber-cavity cases $\xi_f = 0.5$ in (a) and $\xi_f = 3$ in (b) with weak cavity-atom couplings $(\xi_A, \xi_B) = (0.4, 0.4)$ and dissipation couplings $\gamma_i = 0.0$.

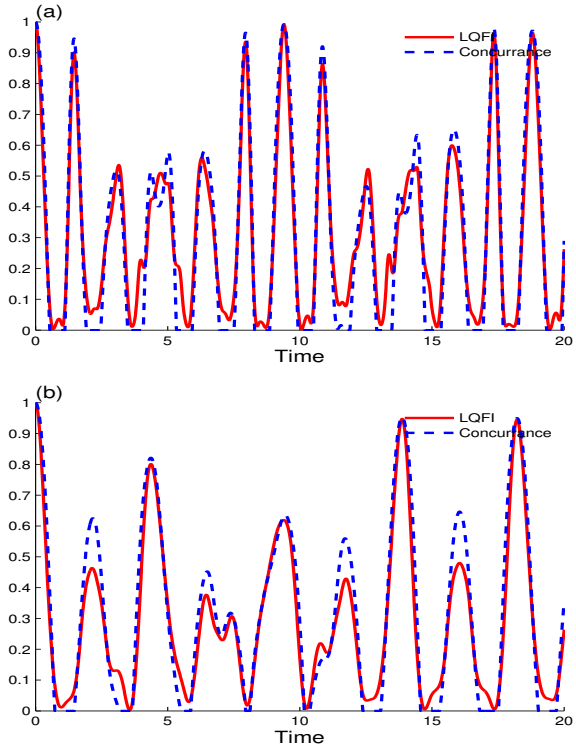

Fig. 5: The dynamics of the atomic local quantum Fisher information and concurrence entanglement of Fig. 4b, but with strong cavity-atom couplings (ξ_A, ξ_B): equal cavity-atom couplings $(\xi_A, \xi_B) = (2, 2)$ in (b), and unequal cavity-atom couplings $(\xi_A, \xi_B) = (2, 0.4)$ in (b).

and the maximal entanglement's concurrence of the initial maximally entangled state: $\frac{1}{16}[|V_2\rangle \otimes |0_A 1_B\rangle + |V_3\rangle \otimes |1_A 0_B\rangle]$ against the increase of the atom-cavity, fiber-cavity, and the two-cavity dissipation couplings.

Fig. 4a shows the dynamics of the maximal coherence's local QFI and the maximal entanglement's concurrence of the initial maximally entangled state: $\frac{1}{16}[|V_2\rangle \otimes |0_A 1_B\rangle + |V_3\rangle \otimes |1_A 0_B\rangle]$ are shown for the fiber-cavity case of $\xi_f = 0.5$ in in the presence of the weak cavity-atom interaction couplings $(\xi_A, \xi_B) = (0.4, 0.4)$ and dissipation couplings $\gamma_i = 0.0$. The coherence's local QFI and the maximal entanglement's concurrence oscillate between their extreme values and regulate to have different periodical oscillatory behaviors. For the weak atom-cavity and fiber-cavity couplings, the maximal initial coherence's local quantum Fisher information and the maximal entanglement's concurrence are loosed and gained their maximal initial coherence and entanglement. Where the two atoms have partial LQFI and entanglement during time intervals and do not have coherence's local quantum Fisher information and the entanglement's concurrence at other times. After a specific time, the atomic coherence's local quantum Fisher information decreases and vanishes instantly, then it revivals and grows to its partial and maximal atomic coherence. While, the entanglement's concurrence vanishes suddenly for a particular time interval, the it revivals suddenly and grows to its partial and maximal entanglement. These phenomena of the sudden death and revival of the two-atom entanglement's concurrence happens, severally, at the ends of the time intervals of the entanglement's concurrence disappearance.

Fig. 4b shows the sensitivity of the dynamics of the generated atomic local QFI and concurrence entanglement due to strong unequal cavity-atom couplings $(\xi_A, \xi_B) = (2, 2)$ combined with the strong fiber-cavity coupling $\xi_f = 3$. In this case, the generated atomic local QFI and concurrence entanglement become more robust with the strong fiber-cavity coupling $\xi_f = 3$. The upper bounds of the local quantum Fisher information are shifted up and the atomic coherence do not vanish. The time intervals of the entanglement's

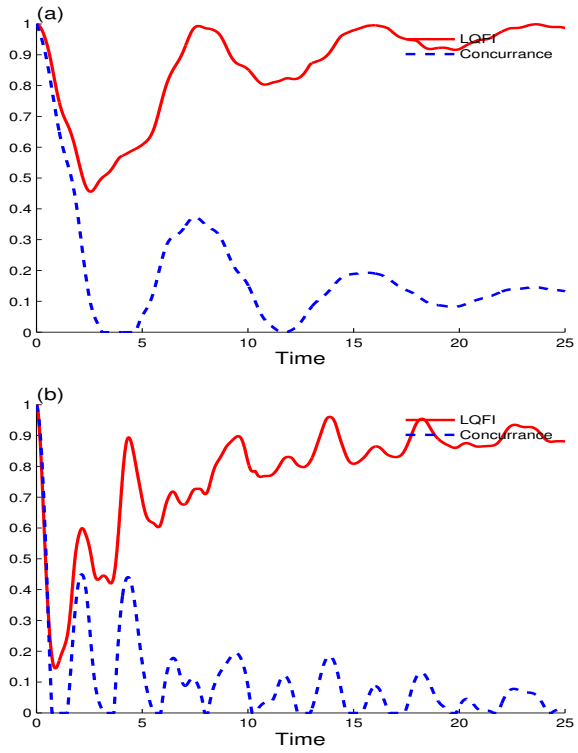

Fig. 6: The atomic local QFI and concurrence entanglement of Figs. 4b and 5b but with strong two-cavity dissipation couplings $\gamma_A = \gamma_B = 0.08$.

concurrence disappearance are reduced. The robustness dynamics of the maximal coherence's local quantum Fisher information and the maximal entanglement's concurrence can be enhanced by increasing the fiber-cavity coupling.

From Fig. 5(a,b), we can find that the strong equal/unequal cavity-atom couplings (ξ_A, ξ_B) lead to weaken the robustness dynamics of the maximal coherence's local quantum Fisher information and the maximal entanglement's concurrence of the initial maximally entangled state: $\frac{1}{16}[|V_2\rangle \otimes |0_A 1_B\rangle + |V_3\rangle \otimes |1_A 0_B\rangle]$ against the increase of the atom-cavity, fiber-cavity, and the two-cavity dissipation couplings. The generate atomic coherence's local quantum Fisher information and entanglement's concurrence have irregular oscillatory dynamics. The LQFI and entanglement frequencies increased and amplitudes decreased. The time disappearance intervals of the atomic entanglement are reduced by increasing th two-cavity dissipation couplings.

In Fig. 6, the atomic local QFI and concurrence entanglement of Figs. 4b and 5b are displayed for strong two-cavity dissipation couplings $\gamma_A = \gamma_B = 0.08$. Fig. 6a shows that the upper bounds of the local QFI amplitudes increase to return its initial maximal value's local QFI by increasing the two-cavity dissipation couplings. While the concurrence entanglement amplitudes degrades and vanishes, completely, due to the two-cavity dissipation effects. While the atomic local QFI grows to stabilizes at maximal atomic coherence, the concurrence reduces to create the time entanglement's concurrence disappearance intervals. For under unequal strong cavity-atom couplings, we observe that the growth of the atomic coherence's local QFI and the degradation of the concurrence entanglement are enhanced. The robustness (against the cavity dissipation and atom-cavity and fiber-cavity couplings) and the stability of the Local QFI growth and the degradation of the concurrence depend on the atom-cavity, fiber-cavity, and cavity dissipation couplings.

5 Conclusion

We explore local quantum Fisher information and concurrence entanglement of two distant qubits interacting separately with two coupled dissipative cavities via an optical fiber. Under increasing couplings of the cavity-atom interaction, fiber-cavity interaction, and cavity dissipation coupling, the generation and robustness of the atomic local QFI and two-atom concurrence quantum information resources have been investigated. It is found that, by increasing the strong fiber-cavity interactions in the presence of the unequal cavity-atom couplings, the frequencies, regularity, and amplitudes of the generation of the atomic local quantum Fisher information and entanglement are enhanced and the time disappearance intervals of the entanglement's concurrence are reduced.The local QFI sudden-changes points enhanced. The atomic entanglement's concurrence exhibits sudden disappearance and sudden reappearance phenomena, severally. The increase of cavity dissipation coupling leads to growth of the atomic coherence's local QFI and the degradation of the concurrence entanglement. The stability of the Local QFI growth and the concurrence degradation depends on the atom-cavity, fiber-cavity, and cavity dissipation couplings. The robustness dynamics of the maximal initial-coherence's local QFI and the maximal concurrence entanglement can be enhanced by increasing the fiber-cavity coupling. The atomic coherence growth's local QFI and the degradation of the concurrence entanglement (due to the against the cavity dissipations) depend on the increase of the cavity-atom couplings. The robustness (against the cavity dissipation and atom-cavity and the fiber-cavity couplings) and the stability of the Local QFI growth and the concurrence degradation depend on the atom-cavity, fiber-cavity, and cavity dissipation couplings.

Conflict of Interest

The authors declare that there is no conflict of interest regarding the publication of this article.

Acknowledgement

The authors extend their appreciation to Prince Sattam bin Abdulaziz University for funding this research work through the project number (PSAU/2023/01/24618).

References

[1] M. A. Nielsen and I. L. Chuang, Quantum Computation and Quantum Information (Cambridge University Press, Cambridge, 2001).
[2] R. J. Glauber, The Quantum Theory of Optical Coherence, *Phys. Rev.* **130**, 2529 (1963).
[3] A. Streltsov, G. Adesso, and M. B. Plenio, Quantum coherence as a resource, *Rev. Mod. Phys.* **89**, 041003 (2018).
[4] E. Chitambar and G. Gour, Quantum resource theories, *Rev. Mod. Phys.* **91**, 025001 (2019).
[5] K.-D. Wu, A. Streltsov, B. Regula, G.-Y. Xiang, C.-F. Li, and G.-C. Guo, *Advanced Quantum Technologies* **4**, 2100040 (2021).
[6] Y. Wu et al., Strong Quantum Computational Advantage Using a Superconducting Quantum Processor, *Phys. Rev. Lett.* **127**, 180501 (2021).
[7] C. Li, N. Jiang, Y.-K. Wu, W. Chang, Y.-F. Pu, S. Zhang, and L.-M. Duan, Quantum Communication between Multiplexed Atomic Quantum Memories,*Phys. Rev. Lett.* **124**, 240504 (2020).
[8] C. Harney, S. Pirandola, Secure Quantum Pattern Communication, *PRX Quantum* **3**, 010311 (2022).
[9] Y. Yang, Memory Effects in Quantum Metrology, *Phys. Rev. Lett.* **123**, 110501 (2019).
[10] S. J. D. Phoenix and P. L. Knight, Periodicity, phase, and entropy in models of two-photon resonance, *J. Opt. Soc. Am.* B **7**, 116 (1990).
[11] V. Buzek, H. Moya-Cessa, P. L. Knight and S. J. D. Phoenix, Schrödinger-cat states in the resonant Jaynes-Cummings model: Collapse and revival of oscillations of the photon-number distribution, *Phys. Rev.* A **45**, 8190 (1992).
[12] A.-B. A. Mohamed, H. Eleuch, and C. H. Raymond Ooi, Non-locality Correlation in Two Driven Qubits Inside an Open Coherent Cavity: Trace Norm Distance and Maximum Bell Function, *Sci. Rep.* **9**, 19632 (2019).
[13] G. Vidal, R. F. Werner, Computable measure of entanglement, *Phys. Rev.* A **65**, 032314 (2002).
[14] W. K. Wootters, Entanglement of Formation of an Arbitrary State of Two Qubits, *Phys. Rev. Lett.* **80**, 2245 (1998).
[15] A.-B. A. Mohamed, H. Eleuch, and C. H. Raymond Ooi, Quantum coherence and entanglement partitions for two driven quantum dots inside a coherent micro cavity, *Phys. Lett. A* **383**, 125905 (2019).
[16] A.-B. A. Mohamed, H. Eleuch, Coherence and information dynamics of a Λ-type three-level atom interacting with a damped cavity field, *Eur. Phys. J. Plus* **132**, 1-8 (2017).
[17] E. P. Wigner, M. M. Yanase, Information Contents Of Distributions, *Proc. Natl. Acad. Sci.* USA **49**, (1963) 910.
[18] D. Girolami, T. Tufarelli, G. Adesso, Characterizing Nonclassical Correlations via Local Quantum Uncertainty, *Phys. Rev. Lett.* **110**, 240402 (2013).
[19] S.-X. Wu, J. Zhang, C.-S. Yu and H.-S. Song, Uncertainty-induced quantum nonlocality, *Phys. Lett.* A **378**, 344 (2014).
[20] C. Radhakrishnan, M. Parthasarathy, S. Jambulingam,and T. Byrnes, Distribution of Quantum Coherence in Multipartite Systems, *Phys. Rev. Let.* **116**, 150504 (2016).
[21] C. Radhakrishnan, M. Parthasarathy, S. Jambulingam, and T. Byrnes, Quantum coherence of the Heisenberg spin models with Dzyaloshinsky-Moriya interactions, *Sci. Rep.* **7**, 13865 (2017).
[22] G. Tóth, Multipartite entanglement and high-precision metrology, *Phys. Rev.* A **85**, 022322 (2012).
[23] Deng-hui Yu and Chang-shui Yu, Quantifying coherence in terms of Fisher information,*Phys. Rev. A* **106**, 052432 (2022).
[24] M. G. Genoni, S. Olivares, M. G. Paris, Fisher-information-based estimation of optomechanical coupling strengths, *Phys. Rev. Lett.* **102**, 013508 (2020).
[25] D. Girolami, A. M. Souza, V. Giovannetti, T. Tufarelli, J.G. Filgueiras, R.S. Sarthour, D. O. Soares-Pinto, I. S. Oliveira, G. Adesso, Quantum Discord Determines the Interferometric Power of Quantum States, *Phys. Rev. Lett.*, **112**, 210401 (2014).
[26] H. S. Dhar, M.N. Bera, G. Adesso, Characterizing non-Markovianity via quantum interferometric power, *Phys. Rev. A*, **991**, 032115 (2015).
[27] A.-B. A. Mohamed, E. M. Khalil, M. F. Yassen and H. Eleuch, Two-Qubit Local Fisher Information Correlation beyond Entanglement in a Nonlinear Generalized Cavity with an Intrinsic Decoherence, *Entropy* **23**, 311 (2021).
[28] R. A. Abdelghany, A.-B. A. Mohamed, M. Tammam and A.-S. F. Obada, Nonclassical correlations in two-qubit Ising model with an arbitrary magnetic field: Local quantum Fisher information and local quantum uncertainty, *Eur. Phys. J. Plus* **136**, 680 (2021).
[29] A-B. A. Mohamed and H. Eleuch, Thermal local Fisher information and quantum uncertainty in Heisenberg model, *Phys. Scr.* **97**, 095105 (2022).
[30] M. A. Yurischev, S. Haddadi, Local quantum Fisher information and local quantum uncertainty for general X states, *Phys. Lett. A* **476**, 128868 (2023).
[31] S. Haseli, Local quantum Fisher information and local quantum uncertainty in two-qubit Heisenberg XYZ chain with Dzyaloshinskii–Moriya interactions, *Laser Phys.* **30**, 105203 (2020).
[32] Z. Dahbi, A. U. Rahman, M. Mansour, Characterization of human mobility based on Information Theory quantifiers,*Physica A* **609**, 128333 (2023).
[33] M. G. A. Paris, Quantum estimation for quantum technology, *Int. J. Quantum Inf.* **7**, 125 (2009).
[34] M. Paternostro, M. S. Kim and G. M. Palma, Non-local quantum gates: A cavity-quantum-electrodynamics implementation, *J. Mod. Opt.* **50**, 2075 (2003).
[35] A.-B. A. Mohamed and H. Eleuch, Quantum correlation control for two semiconductor microcavities connected by an optical fiber,*Phys. Scr.* **92**, 065101 (2017).
[36] A. Serafini, S. Mancini, and S. Bose, Distributed Quantum Computation via Optical Fibers *Phys. Rev. Lett.* **96**, 010503 (2006).

[37] S. Clark, A. Peng, M. Gu, and S. Parkins, Unconditional Preparation of Entanglement between Atoms in Cascaded Optical Cavities, *Phys. Rev. Lett.* **91**, 177901 (2003).
[38] L.-M. Duan and H. J. Kimble, Efficient Engineering of Multiatom Entanglement through Single-Photon Detections,*Phys. Rev. Lett.* **90**, 253601 (2003).
[39] A.-B. A. Mohamed and H. Eleuch, Generation and robustness of bipartite non-classical correlations in two nonlinear microcavities coupled by an optical fiber, *J. Opt. Soc. Am.* B **35**, 47 (2018).
[40] E. A. Sete and H. Eleuch, Fast fault-tolerant decoder for qubit and qudit surface codes, *Phys. Rev.* A **9** 032309 (2015).
[41] A.-B. A. Mohamed, Control of Quantum and Classical Correlations in Werner-Like States of Two-Qubit Cavity System under Dissipative Environments, *Appl. Math. Inf. Sci.* **9**, 2997-3002 (2015).
[42] A.-B. A. Mohamed, Quantum discord and its geometric measure with death entanglement in correlated dephasing two qubits system, *Quant. Inf. Rev.* 1, **1**, 1-7 (2013).
[43] X. Y. Yu, J. H. Li and X. B. Li, Generation of maximally entangled state from a single-photon state in fiber-connected cavities, *Optik* **124**, 5723 (2013).
[44] S. L. Su, X. Q. Shao, Qi Guo, L. Y. Cheng, H. F. Wang and S. Zhang, Training Schrödinger's cat: quantum optimal control, *Eur. Phys. J.* D **69**, 123 (2015).
[45] I. M. Mirza, Dynamics of strongly driven two-level systems: analytical solutions, *Phys. Lett.* A **379**, 1643 (2015).
[46] W. H. Louisell: *Quantum Statistical Properties of Radiation*. Wiley, New York (1973)
[47] H. Eleuch, Photon statistics of light in semiconductor microcavities, *J. Phys. B: At. Mol. Opt. Phys.* **41**, 055502 (2008).
[48] A.-B. A. Mohamed and H. Eleuch, Non-classical effects in cavity QED containing a nonlinear optical medium and a quantum well: Entanglement and non-Gaussanity, *Eur. Phys.* J. D **69**, 191 (2015).
[49] A. Serafini, S. Mancini and S. Bose, Distributed Quantum Computation via Optical Fibers, *Phys. Rev. Lett.* **96**, 010503 (2006).

A.-B. A. Mohamed received the M.S. and Ph.D. degrees in applied mathematics from Assiut University, Egypt. He is currently a Professor with Assiut University and Prince Sattam Bin Abdulaziz University, Saudi Arabia. From 2019, he is professor of Mathematics, Assuit University, Egypt. And From 2018, he is Professor of Mathematics, Prince Sattam Bin Abdulaziz Un., KSA. His research interests include applied mathematics and mathematical physics, including different directions in quantum information and computation.